Climate change projection of snowfall in the Colorado River Basin using dynamical downscaling

Sungwook Wi,[1] Francina Dominguez,[2,3] Matej Durcik,[3] Juan Valdes,[1,3] Henry F. Diaz,[4] and Christopher L. Castro[2]

Received 15 March 2011; revised 8 March 2012; accepted 18 March 2012; published 3 May 2012.

[1] Recent observations show a decrease in the fraction of precipitation falling as snowfall in the western United States. In this work we evaluate a historical and future climate simulation over the Colorado River Basin using a 35 km continuous 111 year simulation (1969–2079) of the Weather Research and Forecasting (WRF) regional climate model with boundary forcing from the Hadley Centre for Climate Prediction and Research/Met Office's HadCM3 model with A2 emission scenario. The focus of this work is to (1) evaluate the simulated spatiotemporal variability of snowfall in the historical period when compared to observations and (2) project changes in snowfall and the fraction of precipitation that falls as snow during the 21st century. We find that the spatial variability in modeled snowfall in the historical period (1981–2005) is realistically represented when compared to observations. The trends of modeled snowfall are similar to the observed trends except at higher elevations. Examining the continuous 111 year simulation, we find the future projections show statistically significant increases in temperature with larger increases in the northern part of the basin. There are statistically insignificant increases in precipitation, while snowfall shows a statistically significant decrease throughout the period in all but the highest elevations and latitudes. The fraction of total precipitation falling as snow shows statistically significant declines in all regions. The strongest decrease in snowfall is seen at high elevations in the southern part of the basin and low elevations in the northern part of the basin. The regions of most intense decreases in snow experience a decline of approximately 50% in snowfall throughout the 111 year simulation period. The regions of strongest declines in snowfall roughly correspond to the region of migration of the zero degree Celsius line and emphasize snowfall dependence on both altitude and latitude.

Citation: Wi, S., F. Dominguez, M. Durcik, J. Valdes, H. F. Diaz, and C. L. Castro (2012), Climate change projection of snowfall in the Colorado River Basin using dynamical downscaling, *Water Resour. Res.*, *48*, W05504, doi:10.1029/2011WR010674.

1. Introduction

[2] The Colorado River Basin encompasses a large geographic area ranging from the high Rocky Mountains of Wyoming and Colorado to the low-lying semiarid deserts of Arizona and Mexico (Figure 1a). Mountain headwater streams of the Colorado River occupy only 15% of the area and supply approximately 85% of the river's 17.2×10^9 m^3 annual flow [*Christensen and Lettenmaier*, 2007; *Serreze et al.*, 1999]. In this region, snow acts as the largest storage of precipitation in the winter, with release of water during the critical spring and summer months [*Mote et al.*, 2005]. Observations over the past 50 years show a decrease in April 1 snow water equivalent (SWE) and a shift to earlier onset of snowmelt-driven streamflow in both the Upper and Lower Colorado River Basins [*Mote et al.*, 2005; *Grundstein and Mote*, 2010; *Stewart et al.*, 2005]. However, high-elevation stations in the Rocky Mountains of Colorado show no trends or positive trends for the SWE and the timing of streamflow [*Mote et al.*, 2005; *Stewart et al.*, 2005]. Observations show that changes in accumulated SWE are due, in part, to the widespread decline in the proportion of precipitation that falls as snow, particularly in the Lower Colorado Basin [*Knowles et al.*, 2006]. Notably, the changes in SWE, SWE/P and timing of snowmelt-driven streamflows cannot be explained by natural variability alone and are likely due in part to climate change induced by anthropogenic greenhouse gas emissions [*Karoly et al.*, 2003; *Bonfils et al.*, 2008; *Pierce et al.*, 2008; *Barnet et al.*, 2008; *Hidalgo et al.*, 2009]. Future hydroclimatologic projections derived from the Coupled Model Intercomparison Project phase 3 (CMIP3) global climate models (GCMs) or their downscaled products, indicate that the Colorado River Basin faces increased

[1]Department of Civil Engineering and Engineering Mechanics, University of Arizona, Tucson, Arizona, USA.
[2]Department of Atmospheric Sciences, University of Arizona, Tucson, Arizona, USA.
[3]Department of Hydrology and Water Resources, University of Arizona, Tucson, Arizona, USA.
[4]NOAA/ESRL/CIRES, Boulder, Colorado, USA.

0043-1397/12/2011WR010674

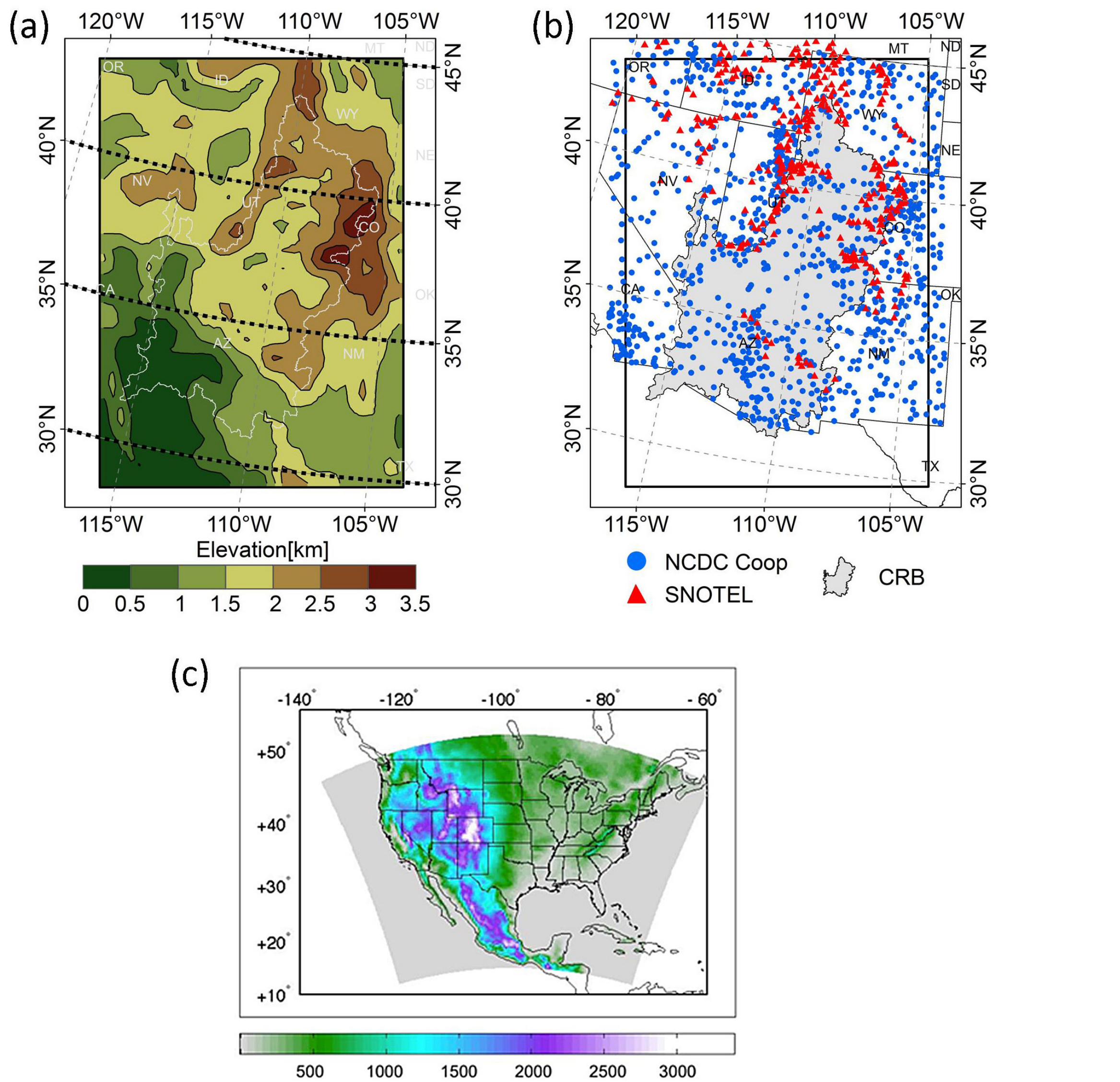

Figure 1. (a) Topographic characteristic of the study domain, including the altitudinal and latitudinal bands used in this study (b) The study domain (Colorado River Basin) with the location of all SNOTEL and NCDC Coop stations where SFE data are available for gridding (c) WRF-model domain, and model representation of topography (m).

temperatures, reductions in land surface runoff in the coming decades [*Milly et al.*, 2005; *Christensen and Lettenmaier*, 2007; *Gao et al.* 2011]. While winter precipitation is projected to increase or remain unchanged for the Upper Colorado, the Lower Colorado is projected to have decreased mean winter precipitation [*Dominguez et al.*, 2012]. Interestingly, projections of decreased runoff using downscaled climate variables are less intense than those predicted by the coarse-scale GCMs primarily due to the finer scale representation of snowpack processes in the headwaters of the Colorado [*Gao et al.*, 2011].

[3] While many studies have looked at observed and simulated effects of warmer temperatures on snowpack in the Colorado River Basin, it is important to keep in mind that climate change affects snowpack in three very distinct ways by (1) changing the fraction of total precipitation that falls as snow, by (2) affecting the timing of snowmelt and by (3) changing the large-scale circulation that can in turn affect the storm tracks. While the fraction of precipitation falling as snow is most affected by wintertime temperatures, changes in snowmelt are more sensitive to springtime temperatures [*Knowles et al.*, 2006]. Furthermore, once snow accumulates on the ground, it is affected by complex interactions including solar radiation, boundary layer dynamics, and changes in albedo. Because of these complexities, the simulation of snowpack evolution is a weakness in many land surface models coupled to climate models [*Rutter et al.*, 2009; *Wang et al.*, 2010; *Barlage et al.*, 2010] and is yet another source of uncertainty in climate change projections. For this reason we take a step back and look only at snowfall and the fraction of precipitation that falls as snow in the Colorado Basin. This also includes changes in snowfall due to changes in large-scale circulation as represented in the downscaled simulation. In this

study we analyze how snowfall and the fraction of precipitation that falls as snowfall in the Colorado River Basin is represented in a downscaled climate simulation for the historical period and how these variables might change under future climate with increased greenhouse gas forcing.

[4] Future climate projections using coarse-scale GCMs provide general temperature and precipitation trends at global and continental scales but these are typically not representative of local climates. GCM projections are particularly inadequate in mountainous regions where the topographical gradients, that control climatic conditions, are not captured by the coarse-scale models [*Leung and Qian*, 2003]. Dynamical downscaling is a physically based method to bring the global scale projections to the regional scale by using a regional climate model (RCM) driven by GCM data. Large multi-institutional dynamical downscaling efforts, such as the "North American Regional Climate Change Assessment Program" (NARCCAP) [*Mearns et al.*, 2009] have created ensembles of future climate projections using different GCM-RCM combinations in 30 year time-slice experiments for both the historical and future periods. When comparing NARCCAP RCM to their host GCM projections in the Colorado River Basin, *Gao et al.* [2011] find that the representation of finer scale physical processes by the RCMs led to improved simulation of surface temperature, snowpack and runoff in this mountainous region. The spatial resolution of the RCM simulation used to dynamically downscale the GCM data plays a very important role in complex terrain, affecting precipitation intensity and the accuracy of snow simulation [*Leung and Qian*, 2003]. In the Colorado headwaters in particular, *Ikeda et al.* [2010] and *Rasmussen et al.* [2011] find that very high resolution RCM simulations (on the order of 6 km) are needed to accurately model accumulated snowfall. The authors find that coarser simulations (above 18 km) generally overestimate low-elevation snowfall and underestimate high-elevation snowfall.

[5] The main goal of this work is to analyze the representation of snowfall and the fraction of precipitation falling as snow in the Colorado River Basin as simulated by a 35 km dynamically downscaled simulation using the regional climate model WRF driven by the HadCM3 GCM for the period 1969–2079 (WRF-HadCM3 henceforth). While *Rasmussen et al.* [2011] suggest simulations on the order of 6 km for the proper representation of snow processes; it is currently computationally prohibitive to run a 111 year continuous simulation at such high resolution. For this reason we expect our simulated snowfall to be biased low at high elevations, and we analyze our simulations with this caveat in mind. In particular we will (1) compare the simulations for the historical (1981–2005) period with observations and (2) evaluate future changes due to projected greenhouse gas warming under an A2 emission scenario. The paper is organized as follows: the data and methods used are presented in section 2. In section 3 we evaluate how realistically the WRF-HadCM3 simulation represents temperature, precipitation and snowfall for the historical period when compared to observations. We then present the WRF-HadCM3 simulated changes in future climate for the basin and analyze how simulated snowfall will change in the future with a detailed analysis of its spatial variability as a function of latitude and elevation. Discussion and conclusions are presented in section 4.

2. Data and Methods

2.1. Observational Data

[6] In this study we use snowfall liquid water equivalent (SFE) to quantify snowfall for the winter period (December–March). Proposed by *Knowles et al.* [2006], SFE is defined as the precipitation totals on the days for which newly fallen snow was recorded. This measure is not to be confused with snow water equivalent (SWE), which is the amount of liquid water contained in the snowpack and is strongly affected by land surface processes. Daily observed winter precipitation, temperature, and SWE are derived from the US Natural Resources Conservation Service Snopack Telemetry (SNOTEL), which provide information since the early 1980s. In addition, precipitation, temperature and snow depth are derived from daily observations at the National Climate Data Center (NCDC) cooperative weather stations (NCDC Coop) U.S. The SFE is derived by taking precipitation on the days when SWE >0 for SNOTEL stations, or snow depth >0 for NCDC Coop stations, and setting SFE to zero when SWE or snow depth $= 0$. It is important to clarify that in the discussion that follows, snowfall and SFE are considered synonymous, although it is possible that SFE overestimates snowfall because on the days when precipitation falls in both the liquid and solid phases all of the precipitation is classified as snow.

[7] The records for precipitation, temperature and derived SFE at NCDC Coop and SNOTEL stations were culled according to two criteria: (1) Stations reporting no more than 10 missing days for any given winter season were used to calculate a climatology for the period 1981–2005. (2) During the climatology period of 25 years, stations reporting more than 12 missing seasons were excluded from the gridding process. This is a similar methodology as the one used by *Knowles et al.* [2006]. As a result, 1320 (978 NCDC Coop, 342 SNOTEL) stations were used to create SFE grid data (These 1320 stations are depicted in Figure 1b as an example to show the spatial distribution of stations used for gridding SFE observations), 1409 (1065 NCDC Coop, 344 SNOTEL) stations were used for gridding precipitation data and 1267 stations (929 NCDC Coop, 338 SNOTEL) were used for gridding temperature data. We compared the observations and model simulations for the "box" seen in Figure 1b, which contains stations outside the Colorado Basin. We also used some stations outside the box to improve the gridding purposes in the edges of the box.

[8] We then applied a quality control procedure to both the Coop and SNOTEL data based on a two-step methodology delineated by *Kunkel et al.* [2005]. In the first step, precipitation and temperature data is culled based on the following criteria: all precipitation values whose anomaly from the monthly mean exceeded five standard deviations (fitted to a Gamma distribution) were flagged. In the second step, we flagged all temperature data larger than 40°C or less than -40°C, and all temperature data whose anomaly from the monthly mean exceeded five standard deviations. Additional data were flagged based on differences with nearby stations (details can be found in the work of *Kunkel et al.* [2005]).

[9] Following the quality control, we gridded the data to be compatible with the WRF-HadCM3 output (35 km

resolution grid) using the synergraphic mapping system (SYMAP) algorithm [*Shepard*, 1984]. SYMAP has been used in several studies as a distance- and direction-weighted interpolation scheme to account for the irregular spatial distribution of the observation sites, [*Maurer et al.*, 2002; *Hamlet et al.* 2005]. During the application of SYMAP to temperature data, the temperature lapse rate of 6.1°C km^{-1} was used to adjust for elevation differences. It is important to keep in mind that, regardless of the gridding process, there are inherent limitations in using point observations to provide reliable area-averaged estimates—particularly for fields with significant spatial variability such as SFE. The average number of point observations may not be representative of the area of the region, and most importantly for SFE, the elevation of the observations may not be representative of the mean elevation we are trying to represent in the area average. For the Colorado River Basin we find that the observations above 2000 m are generally located at higher elevations than the average of the region we are representing, and below 2000 m, the observations are generally located at lower elevations (Figure 2).

[10] We also compare the model-derived spatial distribution of precipitation and temperature with the Parameter-Elevation Regressions on Independent Slope Models (PRISM) database (available online at www.prism.oregonstate.edu). PRISM interpolates precipitation and temperature based on elevation, terrain-induced transitions, coastal effects and the persistence of climatic patterns [*Daly et al.*, 1994]. SFE data is unfortunately not available through PRISM.

2.2. Model Data

[11] Future climate projections at the global scale are used as forcing data for the regional climate model. Global 6 hourly forcing data was obtained from the HadCM3 model with A2 emission scenario forcing for 43 vertical levels at an approximate horizontal resolution of 3.75° by 2.5°. These data are the same used to force the regional climate models (RCMs) participating in the NARCCAP

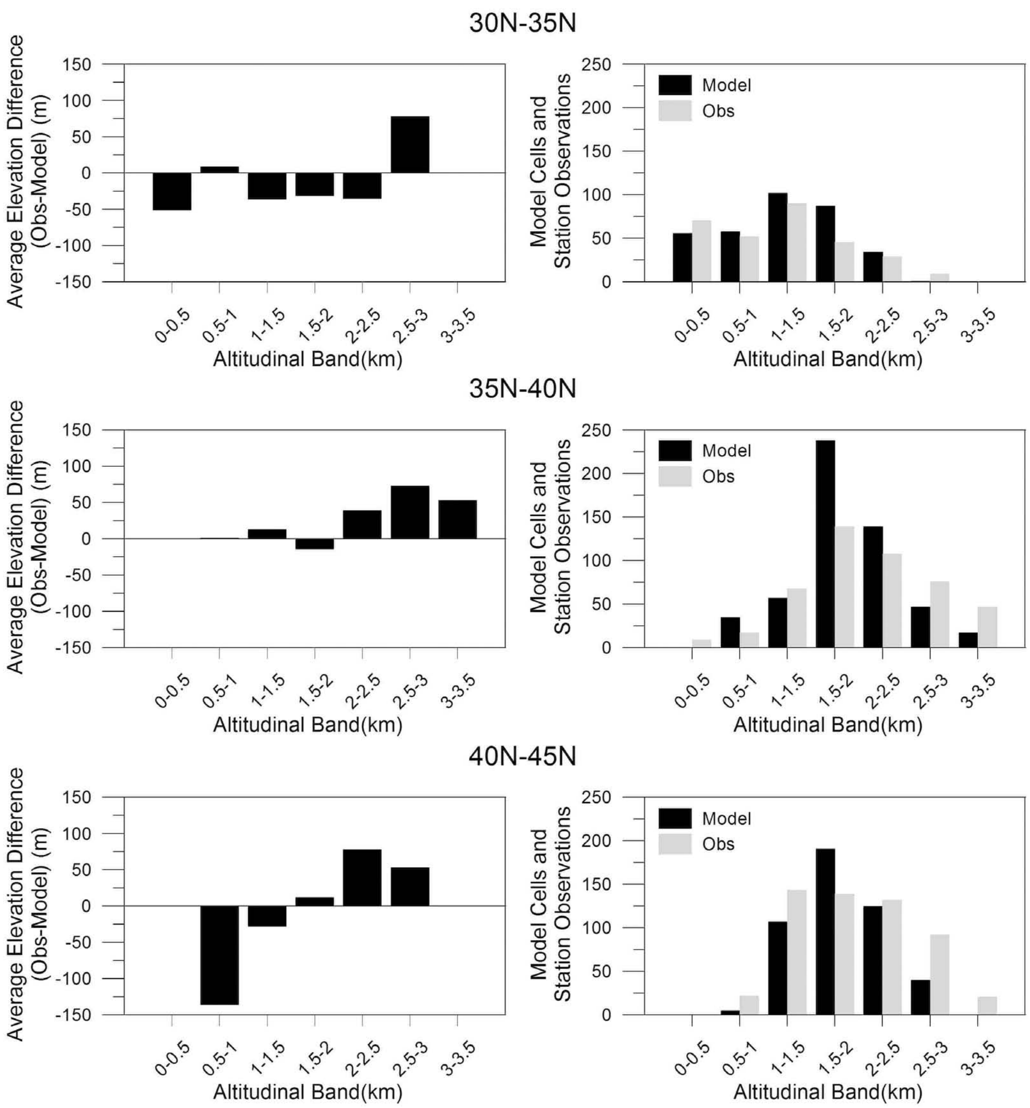

Figure 2. (left) Difference between the average elevation of the observation stations and the average elevation of the model grid cells for each latitudinal and altitudinal band. (right) Number of model grid cells (black) and observation stations (gray) for each latitudinal and altitudinal band.

project. The HadCM3 model has been shown to perform well in the Southwest, realistically capturing the precipitation and temperature in the region, as well as the atmospheric circulation and ENSO interannual variability [*Dominguez et al.*, 2009]. Notably, the HadCM3 was among the models shown by *van Oldenborgh et al.* [2005] to have the most realistic description of the mechanisms of ENSO in the current climate, and this is an important consideration given the strong influence of ENSO-PDO on precipitation variability in the western U.S.

[12] The HadCM3 global data was used as forcing for the Advanced Research version (ARW) of the Weather Research and Forecasting (WRF) regional climate model [*Skamarock et al.*, 2005]. The model was run continuously for 111 years at a 35 km resolution, input to the model was done every 6 h and model output is stored every 6 h. The model domain includes the entire conterminous United States and northern Mexico (Figure 1c); however, in this work we will focus solely on the Colorado River Basin region. The model physical parameterizations are approximately consistent with the options used for real-time high resolution (1.8 km) operational forecasts produced within the Department of Atmospheric Sciences at the University of Arizona, and these include: WRF Single-Moment three-class microphysics [*Hong et al.*, 2004], Kain-Fritsch cumulus parameterization [*Kain and Fritsch*, 1993], Goddard Shortwave radiation [*Chou and Suarez*, 1994], Rapid Radiative Transfer Model (RRTM), Longwave [*Mlawer et al.*, 1997], Eta surface layer [*Janic*, 1996, 2002], Mellor-Yamada-Janic (MYJ) planetary boundary layer [*Janic*, 1990, 1996, 2002], and the Noah land surface model Version 1.0 [*Chen and Dudhia*, 2001]. To ensure the maintenance of synoptic-scale circulation features, like ridges and troughs, in the RCM, spectral nudging is employed in the interior of the domain consistent with *Miguez-Macho et al.* [2004]. Without spectral nudging, the WRF model in a RCM mode can lose variability at the resolved spatial scales of the driving global model, and this behavior is found in other RCM studies [e.g., *Castro et al.*, 2005; *Rockel et al.*, 2008]. We performed spectral nudging on the zonal and meridional winds, the temperatures and the geopotential height fields for all pressure levels below 0.36 of the surface pressure (for a surface pressure of 1000 mb it would be all pressures below 360 mb)—effectively nudging only at very high elevations above the surface. We extract model simulated snowfall on the ground as the WRF variable "snownc" which is the accumulated total snow and ice within the grid, and used this variable without any modification (no bias correction).

2.3. Statistical Analysis

[13] We used the linear regression and Mann–Kendall test [*Kendall*, 1975] to analyze the trends in the observed and simulated hydroclimatic variables. The magnitude of the trends was evaluated with the slopes of the linear regression lines derived from the least squared method, while the statistical significance was determined by the Mann–Kendall trend test. As one of the widely used nonparametric tests to detect trend significance in time series, the Mann–Kendall trend test has been used for a variety of hydroclimatic variables such as temperature, precipitation, streamflow, and evaportranspiration [*Lettenmaier et al.*, 1994; *Zhang et al.*, 2001; *Xu et al.*, 2005; *Burns et al.*, 2007; *Rose*, 2009; *Rio et al.*, 2010]. In this study, we used a p value of 0.05 to identify the statistical significance in trend. The null hypothesis—the assumption there is no trend, was tested with respect to the Mann–Kendall's tau statistics whose distribution follows a normal distribution.

3. Results

3.1. Comparison With Observations

[14] WRF-HadCM3 simulations for the 20th century were compared to observations during the concurrent (1981–2005) time period. It is important to emphasize that GCMs are fully coupled models that include ocean-land-atmosphere interactions and interannual variability will not directly correspond to the observed record. For example, an El Niño year in the observational record will not necessarily correspond to the same specific El Niño event in the simulation. However, as previously mentioned, HadCM3 is a "well performing" GCM in that it reasonably captures ENSO and its associated precipitation anomalies over North America [*Joseph and Nigam*, 2006]. Comparison with observations in a climatological sense is a key step to evaluate the strengths and weaknesses of the model simulation. Our study is focused on the Colorado River Basin, where we compare the model results with data from quality controlled SNOTEL and NCDC observational stations located throughout the region (Figure 1b).

[15] Observations of average winter (December–March) temperature climatology of the region show a clear latitudinal decrease, with average winter temperatures of about 15°C in the southwestern part of the region and close to −10°C in the northeast (Figure 3). The simulation nicely captures the spatial temperature gradient, with a cold bias the region, and in particular in the northeastern part of the region. Precipitation and snowfall are closely tied to topographical forcing, and the simulation captures both the location and intensity of the precipitation distribution, however, there is a generalized overestimation at lower elevations as compared to observations, particularly over Nevada. Note that over the northwestern part of the domain, PRISM shows lower precipitation intensity than the gridded station data.

[16] Focusing specifically on snowfall, we subdivided the region into three 5° latitudinal bands, and seven 500 m altitudinal bands (see Figure 1a), and compared the area-average seasonal winter snowfall between the WRF-HadCM3 (blue), the raw HadCM3 (black) and observations (red) (Figure 4). The raw GCM data was interpolated to the 35 km resolution WRF grid for comparison by replacing a value of regional model grid cell with a value of GCM grid cell which covers a center of the regional model grid cell. We see that, in general, the WRF-HadCM3 has a realistic representation of the average snow with respect to both altitude and latitude. The simulated snowfall from the raw HadCM3 shows that the GCM dramatically underrepresents the altitudinal variability in snowfall, particularly in the northern parts of the basin, showing very high snowfall at low elevations and low snowfall at high elevations, this nicely illustrates the added value of the dynamical downscaling.

[17] While temporally averaged data gives us an idea of how the model captures the mean spatial distribution of snowfall, we are also interested in the temporal variability of temperature, precipitation, snowfall and the ratio

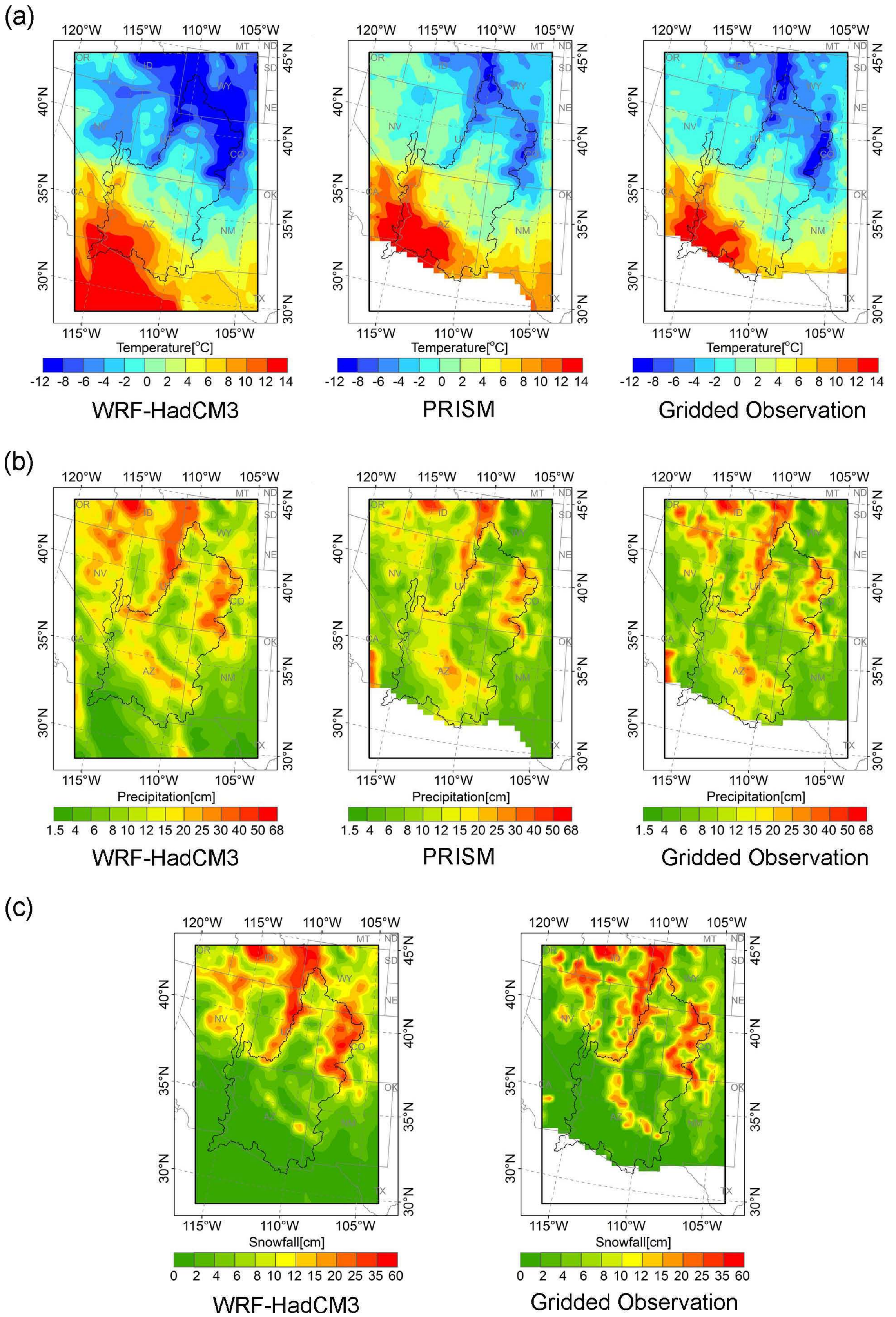

Figure 3. Comparison of model (WRF-HadCM3) climatology for the period 1981–2005 winter (December–March), PRISM and point observation regridded to 35 km. Climatology comparison for (a) temperature, (b) precipitation, and (c) snowfall.

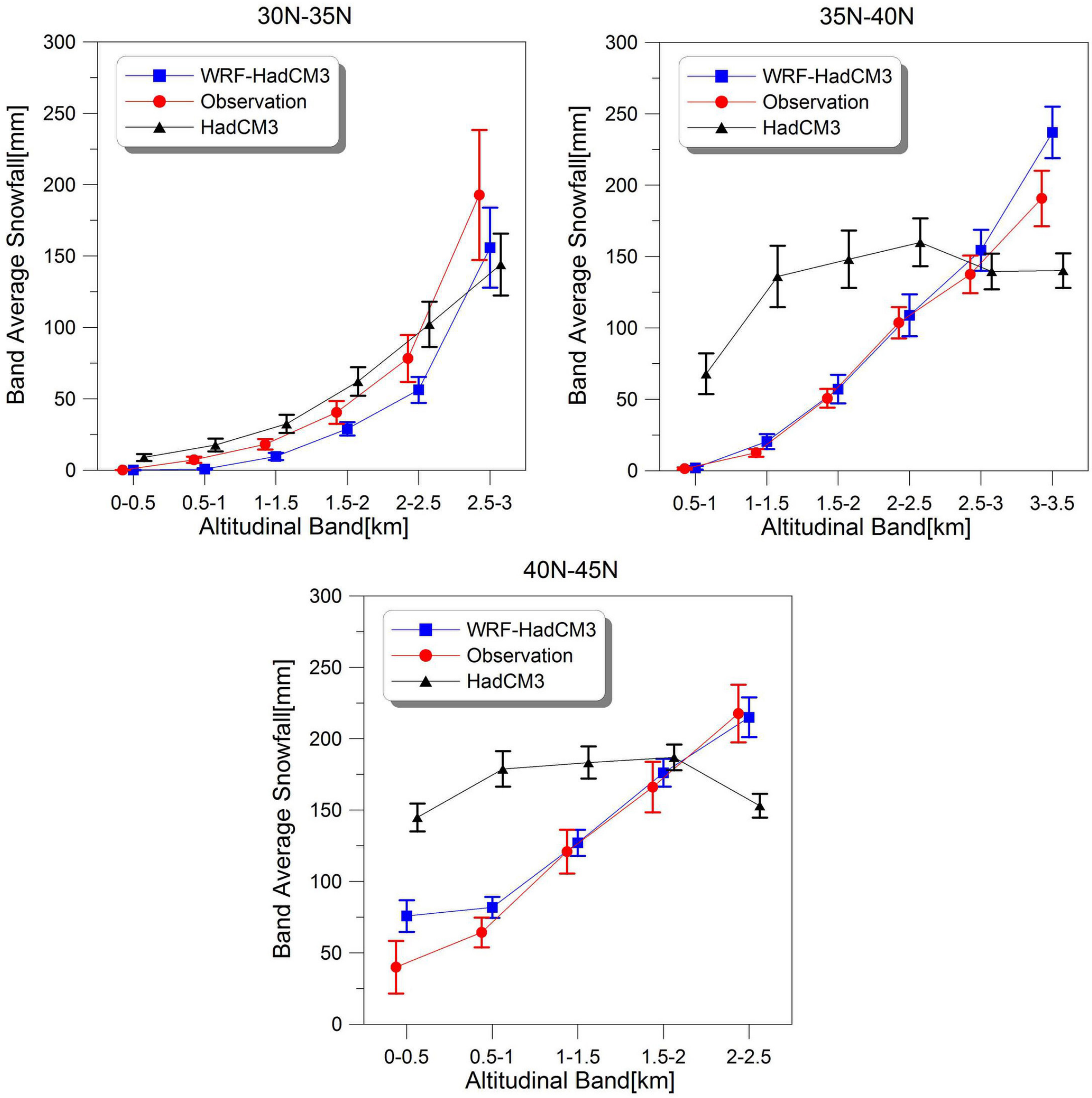

Figure 4. Comparison of model-derived snowfall for the period 1981–2005 winter (December–March) to observed snowfall for three different latitudinal bands and seven altitudinal bands. Each period is averaged in space, and shows total snowfall for the winter (December–March) season.

snowfall/precipitation during the historical period (1981–2005) and how they compare with the simulations. Temperature trends are positive, and mostly not significant, for all bands in the observations and in the simulation (Figure 5). The WRF simulated snowfall trends agree with the sign of the observed trends for all bands except the highest elevations in the two northern bands. As reported in the work of *Knowles et al.* [2006], observations show that many regions in the Rocky Mountains over Colorado and New Mexico have increasing snowfall trends. The model shows small decreasing trends in this high-elevation region, but these trends are not statistically significant. The model has difficulty capturing the mean and interannual variability of snowfall in the 35°N–40°N band, as both are overestimated (Figure 5). The model better captures the mean and interannual variability of snowfall in the two other latitudinal bands, except at the lower elevations. As reported in the work of *Knowles et al.* [2006], we see that many of the observed snowfall trends are not statistically significant (p values of Mann Kendall statistics less than 0.05 are considered to be statistically significant).

[18] Precipitation trends are not statistically significant in any of the latitude-altitude bands (Figure 6), and we see discrepancies between the observed and modeled trends—particularly in the southern part of the domain. On the other hand the modeled and observed trends in SFE/P largely agree, although there are discrepancies at the highest elevations. In general we see that the observed and modeled trends for all variables is generally not statistically significant for the historical period.

3.2. Future Projections

[19] The projections for the future show increased temperatures with larger increases in the northern part of the

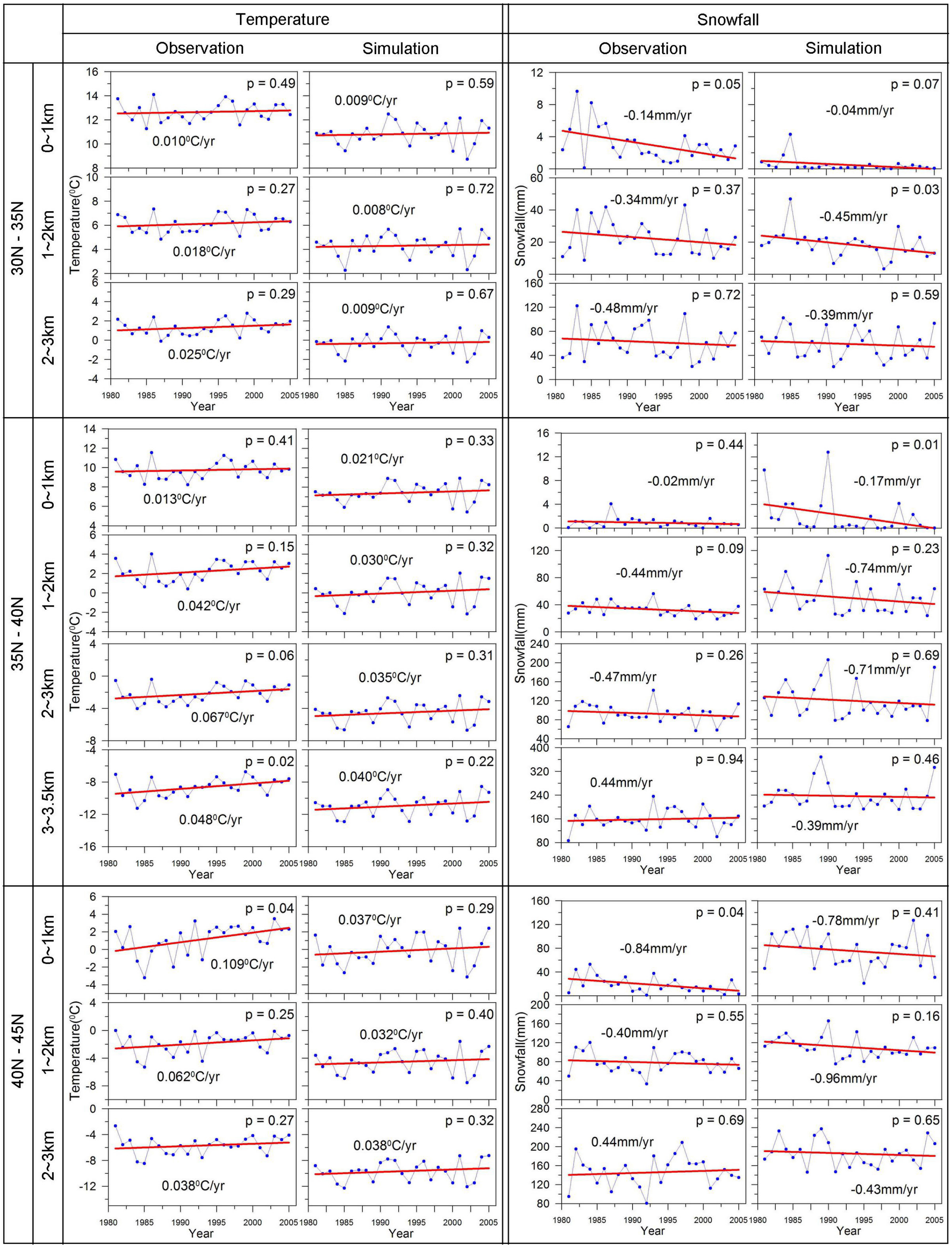

Figure 5. Trend in observed and modeled winter (December–March) area-averaged temperature (left) and snowfall (right) over each of the latitudinal and altitudinal bands. Each panel shows the linear trend and the significance of the trend from Mann Kendal test (p values of Mann Kendall statistics less than 0.05 are considered to be statistically significant).

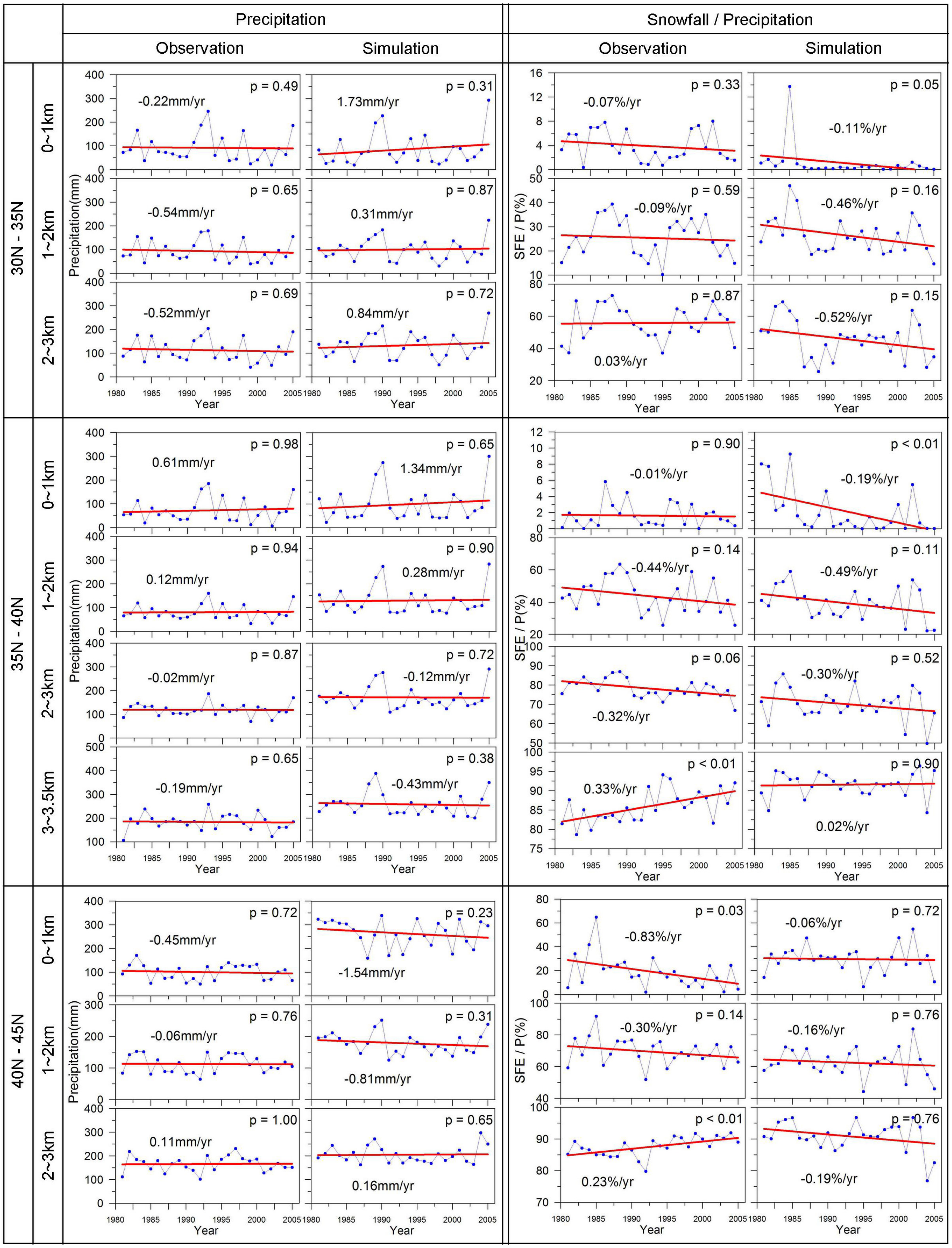

Figure 6. Same as Figure 5 but for precipitation (left) and the ratio of snowfall/precipitation (right).

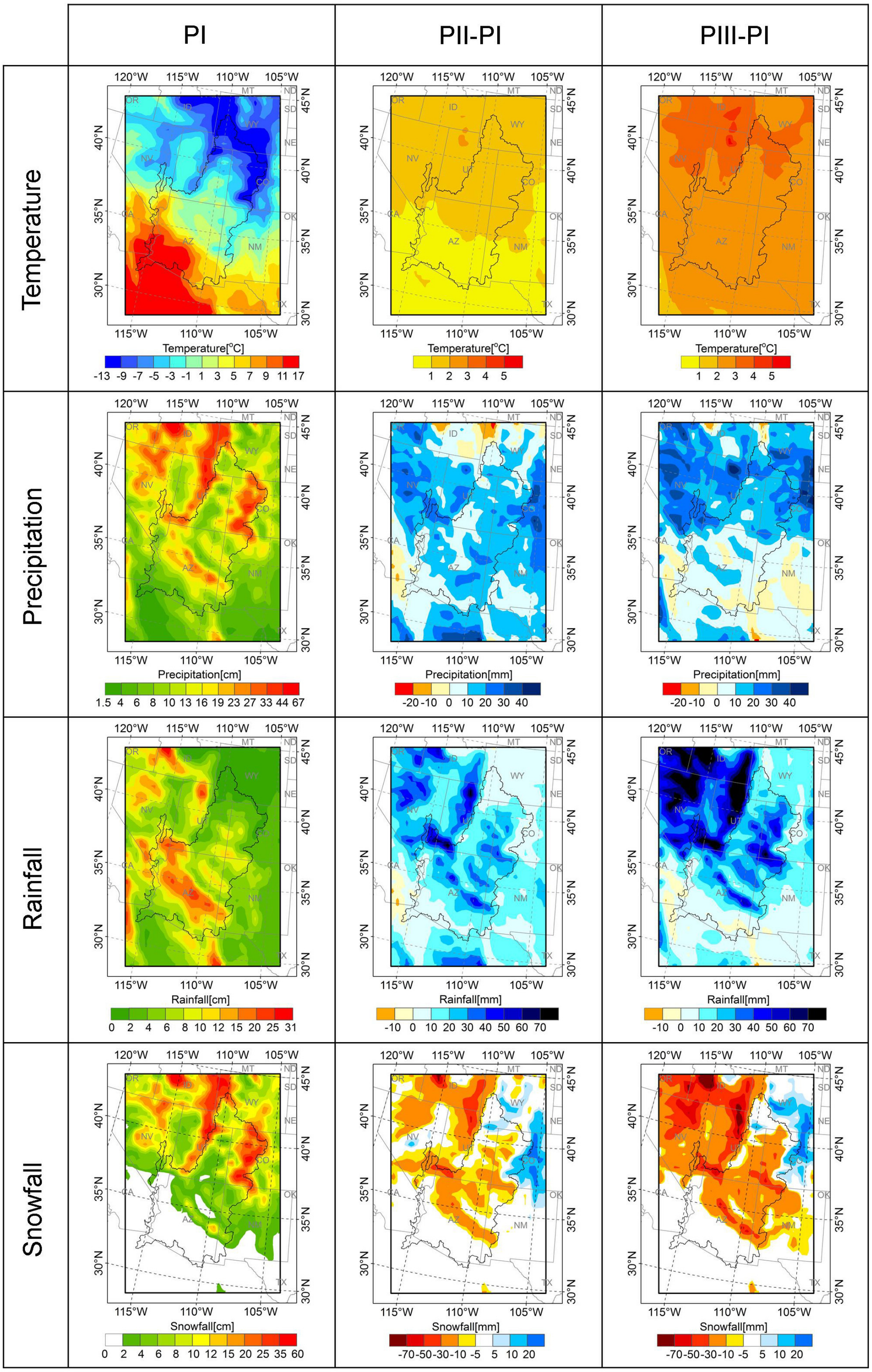

Figure 7. Mean winter (December–March) temperature, precipitation, rainfall and snowfall maps derived from the WRF-HadCM3 simulation. (left) Spatial distribution for the historical period 1969–2005 and (middle) differences between the average 2006–2042 (PII) and PI and (right) differences between 2043–2079 (PIII) and PI.

basin (Figure 7). Mean winter temperatures are projected to increase about 0.35°C/decade. Precipitation changes are spatially heterogeneous and mostly positive throughout the domain, particularly in the northern part of the basin and during the 2006–2042 (PII) period. (Figure 7, second row). Changes in rain are largely positive, and we see a dramatic increase in the rainfall in the northwestern part of the region, an area where there are projected decreases in snowfall (Figure 7, third and fourth rows).

[20] The projections show a decrease in snowfall throughout most of the basin in the coming century, particularly during the 2043–2079 period; however, we do see increasing snowfall in the high elevation in the northeastern part of the domain (Figure 7, fourth row). Interestingly, the high-elevation Colorado Rockies show increasing snowfall while the mountainous regions of Utah, Wyoming and Idaho in the northwestern border of the basin show strong decreasing snowfall. Our hypothesis is that the different altitudes of these ranges and different precipitation projections drive the different response.

[21] The long-term changes over the entire 111 year simulation period reveal large trends in both SFE and the ratio of SFE to total precipitation (SFE/P) (Figure 8). All trends are tested for significance using the Mann–Kendall test and the results of this test are shown for each altitudinal-latitudinal band. Snowfall shows large interannual variability superimposed on trends that are negative and statistically significant for all the latitudinal and altitudinal bands, except the highest elevations of the 35–40°N and 40–45°N bands. This is indicating that only the highest altitudes and

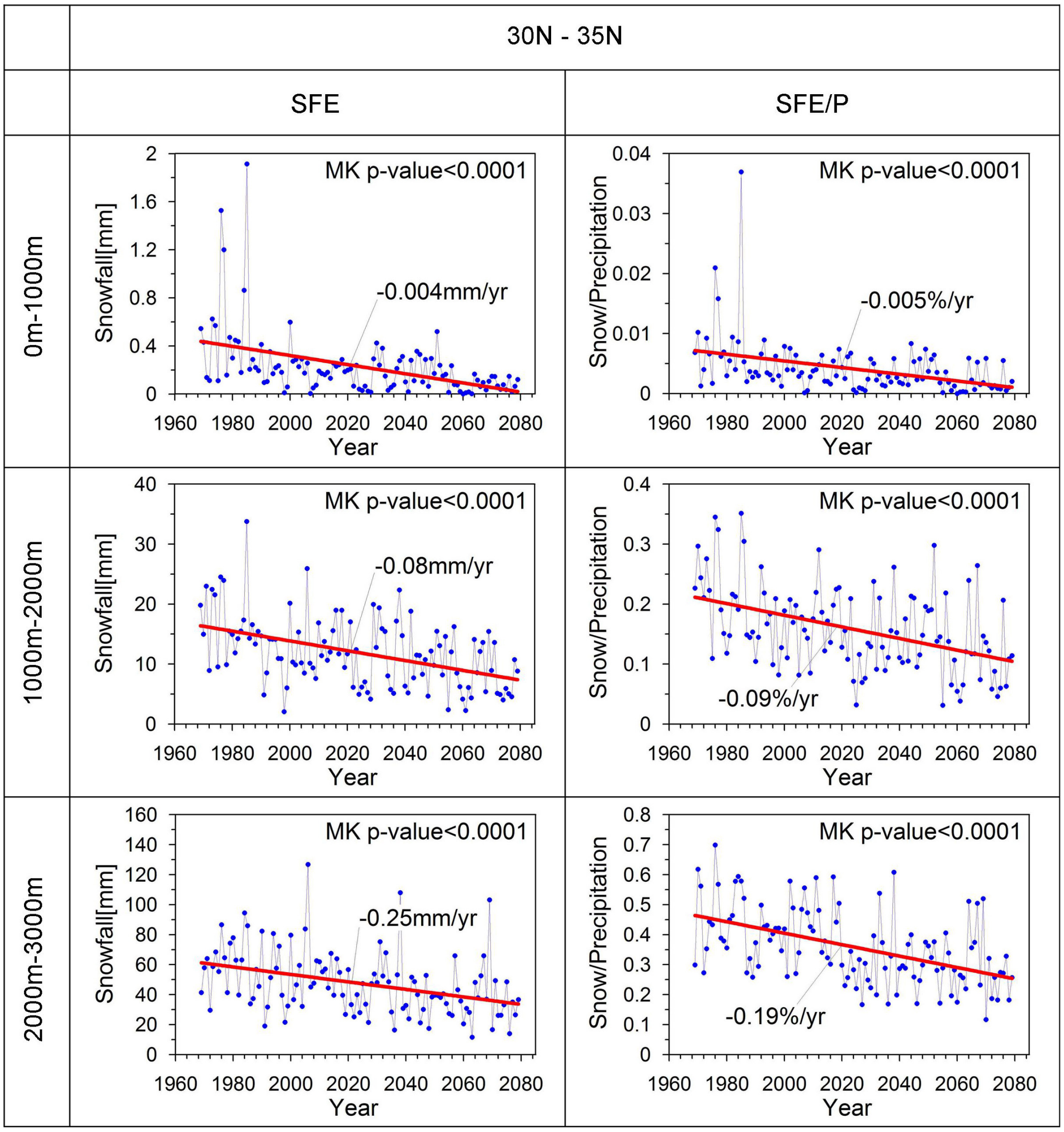

Figure 8. Trends in winter (December–March) SFE and SFE/P for the period 1969–2079 derived from the WRF-HadCM3 simulation. The time series are area-averaged over latitudinal and altitudinal bands. The linear trend and the statistical significance of the trend calculated using the Mann–Kendall test are shown in each panel.

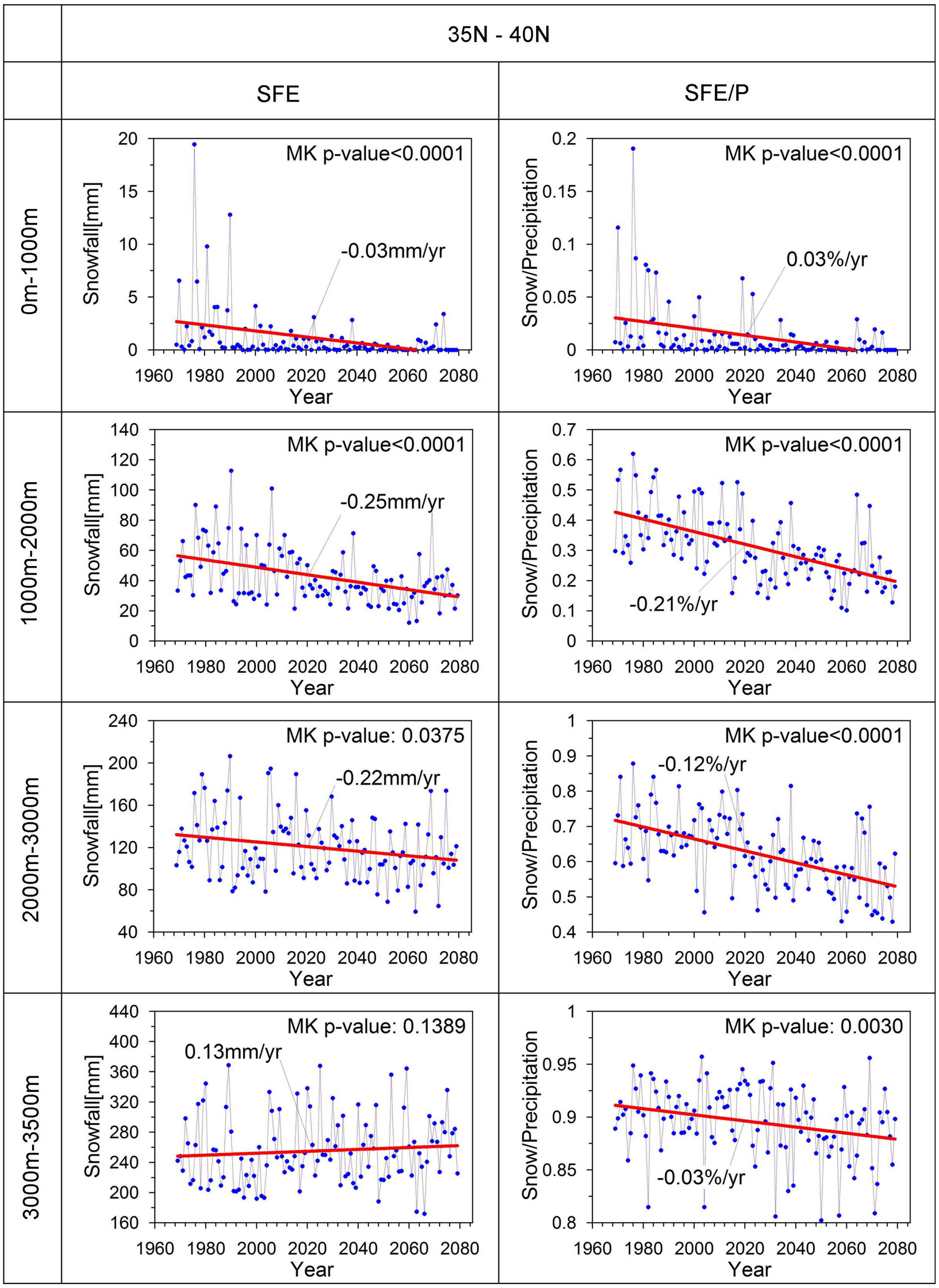

Figure 8. (continued)

latitudes within the Colorado River Basin will likely not see a decrease in snowfall, as increases in snowfall offset increases in temperature. The ratio of snow to total precipitation shows a statistically significant decrease for all elevations and latitudinal bands.

[22] The slope of the linear regressions shown in Figure 8 gives us an idea of the intensity of the projected changes. The slope shows distinct variability in latitude and altitude that can be more easily visualized in Figure 9. As discussed above, the temperature has stronger increases with higher latitudes and the trend is significant throughout the region (there are no hatched areas). Largest increase in temperature is seen at middle attitudes of the northern basin. Precipitation shows generally positive trends with stronger

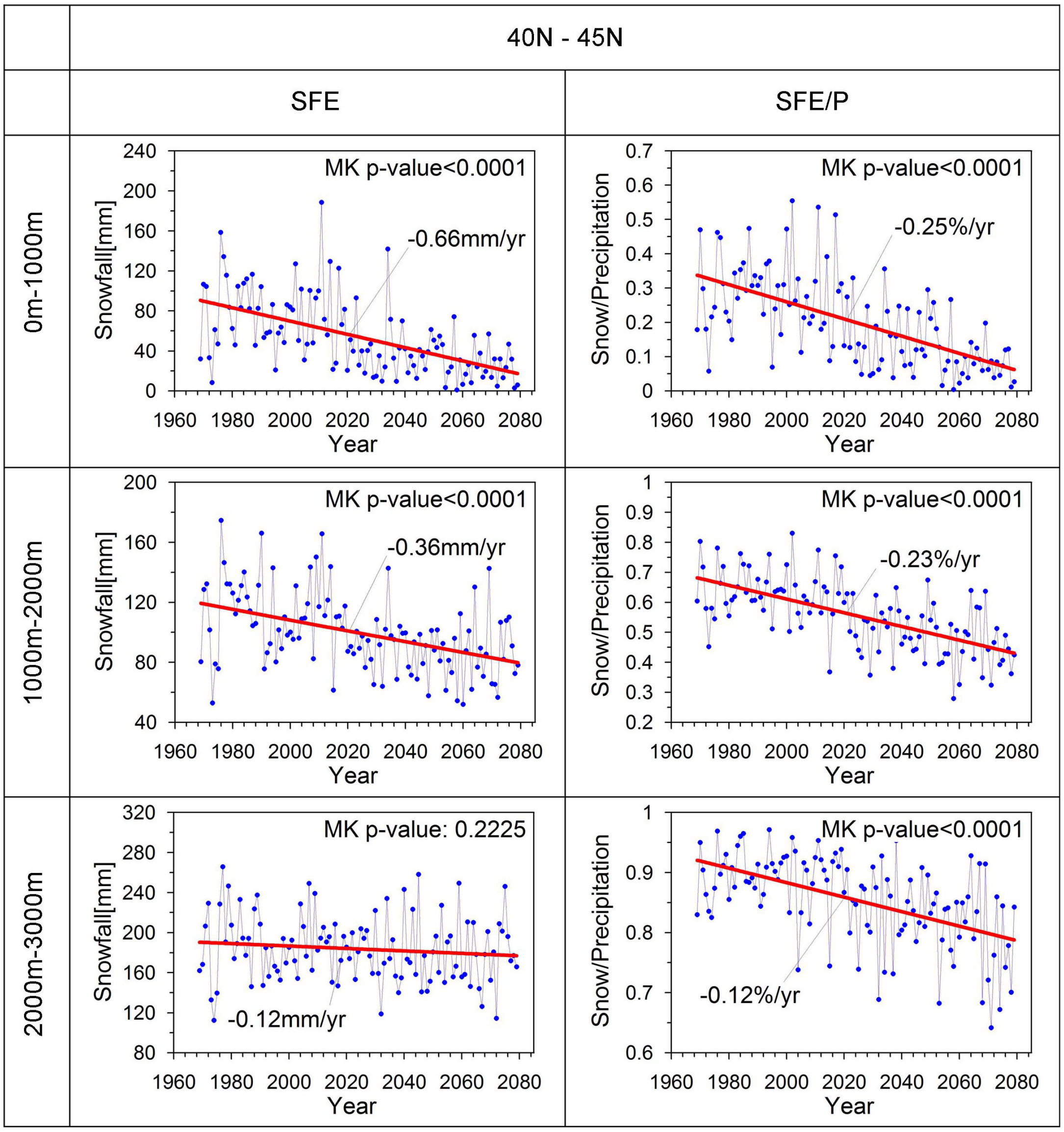

Figure 8. (continued)

positive trends in the lower elevations to the north of the basin. Throughout most of the region the precipitation trends are not statistically significant. Snowfall shows a distinct pattern, where both an altitudinal and latitudinal variation of the slope is evident. The strongest decrease in snow is seen at high elevations in the south and low elevations in the north of the basin. As the results show, the fastest declines in the downscaled projections occur at the higher elevations in Arizona and New Mexico, while Colorado, Utah and Wyoming may see strong snowfall decreases at middle to lower elevations. The trends in snowfall are not statistically significant in the highest elevations (above 2500 m) for latitudes north of 36°N. The regions of most significant declines experience a decrease of approximately 50% in snowfall between the beginning and the end of the simulation (111 years). The snowfall/precipitation trends are significant throughout the region, except in the southernmost low latitudes (these might be a problem with the very small sample size of snow-covered regions in this band). The positive P trend at high elevations and latitudes compensates for nonsignificant SFE trends in the region for a significant decrease in the SFE/P ratio.

4. Discussion and Conclusions

[23] Snow accumulation in the Colorado River Basin is of vital importance for water resources in the region, where the vast majority of the river's streamflow originates as snowmelt. The impacts of warmer temperatures on snow accumulation in this semiarid region are already being observed, and will very likely continue as the region warms. Climate change affects snowpack in three distinct ways by (1) changing the fraction of total precipitation that falls as snow, by (2) affecting the timing of snowmelt and by (3) changing the large-scale circulation patterns that can in turn affect the stormtracks. Given the large uncertainties

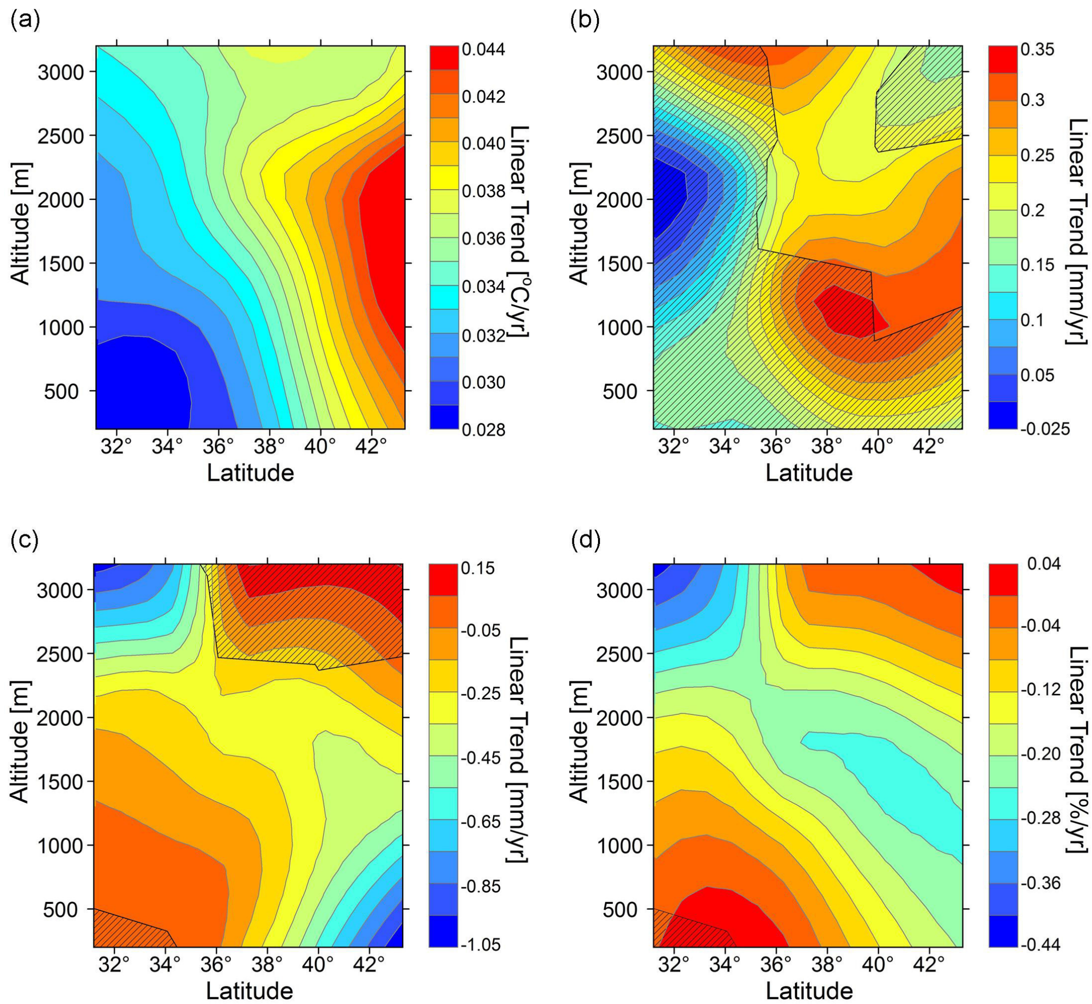

Figure 9. Liner trend of winter (December–March) (a) temperature (°C yr^{-1}), (b) precipitation (mm yr^{-1}), (c) snowfall (mm yr^{-1}), and (d) snowfall/precipitation (% yr^{-1}) for the period 1969–2079 as a function of altitude and latitude. Hatching corresponds to the regions where the trend is not significant.

in simulating snowpack evolution in land surface models, we take a step back and focus only on snowfall (defined as SFE in this study) and the fraction of precipitation that falls as snow (SFE/P). These changes in snowfall include changes in large-scale circulation as represented by the downscaled simulation.

[24] This work analyzes how snowfall and the ratio SFE/P in the Colorado Basin is represented in one downscaled climate model simulation in the historical period and in the future, under an SRES A2 emission scenario. It is important to keep in mind that this work relies on a projection from a single downscaled simulation, and the results should be viewed as model specific. A better idea of model uncertainty will benefit from future additional simulations and comparisons to this work that incorporate different magnitudes of warming, direction and magnitude of precipitation change and different spatial patterns. We hypothesize that the overall trend in snowfall derived from a multimodel comparison would be similar to the one found here due to the temperature dependence, but the spatial and temporal variability would be different due to the snowfall's dependence on precipitation.

[25] A comparison of the WRF-HadCM3 simulation with observations was a critical first step to gain credibility in the model estimates. The climatology of temperature, precipitation and snowfall modeled by WRF-HadCM3 shows a similar spatial pattern to observations, albeit, with underestimations in temperature and overestimations in total precipitation and snowfall. Overestimation of precipitation seems to be a consistent problem with downscaled simulations for the region [*Wang et al.*, 2009]. Comparison with observations also shows that the regional climate modeling is a useful tool to downscale future climate projections in this topographically complex terrain, and adds significant value when compared to the driving HadCM3 GCM. As shown in our results, the coarse resolution of the GCM is inadequate for representing the altitudinal variability in snowfall.

[26] When comparing the observed and modeled temporal variability of snowfall for the historical period, we find that dynamically downscaled snowfall trends for each altitudinal and latitudinal band in the historical period have the same sign as the trends in the observations except at the highest elevations in the northern part of the domain. As

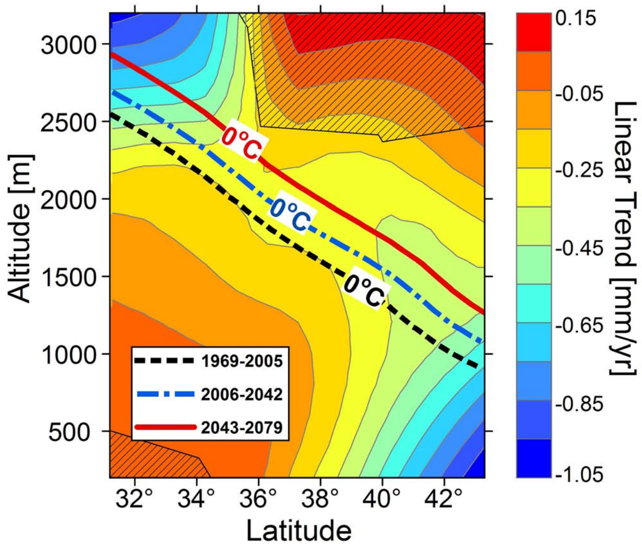

Figure 10. Latitudinal and altitudinal location of the region of zero degree mean winter (December–March) temperature for the three study periods, superimposed on the contours of the linear trend in winter (December–March) snowfall over the period 1969–2079.

stated in the introduction, the 35 km resolution is still too coarse to represent the temporal variability of snowfall at the highest elevations, as was shown in the work of *Ikeda et al.* [2010] and *Rasmussen et al.* [2011], but makes the simulation computationally feasible. Consequently, the simulations have a low-snowfall bias due to the resolution of the simulations and this will also affect the interannual variability. We do not see a low bias in mean snowfall in the Upper Colorado Basin, and this is likely due to the cold model bias. In general, the latitudinal and altitudinal variations in model-derived snowfall versus observed snowfall are similar given all the potential sources of discrepancy. We must keep in mind that the model is not driven by observed sea surface temperatures or circulation, but by fully coupled GCM simulations. In addition, despite the quality control and gridding algorithms, there are difficulties when upscaling point measurements of snow (which is extremely heterogeneous in space and time) to a 35 km grid cell. The fraction of precipitation that falls as snow is dependent upon different parameterizations in the climate model including cloud microphysics, boundary layer, surface layer and land-surface processes, all of which have deficiencies. Finally, there are well known issues with measured snow from an observational standpoint, including catch efficiency [*Knowles et al.*, 2006]. Given all these caveats, WRF-downscaled simulation performs reasonably well in representing the spatiotemporal variability of snowfall.

[27] The dynamically downscaled simulation projects a strong increase in winter temperatures throughout the 111 years, with more significant trends the northern part of the basin. Stronger trends at higher latitudes are seen in the parent HadCM3 GCM [*Dominguez et al.*, 2009], and this pattern is also clear in the multimodel GCM ensemble for the Northern Hemisphere [Intergovernmental Panel on Climate Change, 2007]. Precipitation trends for the 1969–2079 period show increases throughout the domain, particularly in the north, but these trends are not statistically significant. It is clear from this analysis that the interannual variability in precipitation is larger than the trend at all latitudes and elevations (this is the reason why the trends fail the Mann–Kendall test). SFE trends for the 1969–2079 period show high variability superimposed on a statistically significant decrease at all except the highest elevations and latitudes within the basin. While high variability is related primarily to precipitation variability, the declining trend indicates that temperature, not precipitation, is driving the continuous decrease in SFE. Interestingly we see that the high-elevation Colorado Rockies show increasing snowfall, in agreement with the results of *Rasmussen et al.* [2011], however, we do not find increases throughout the headwater region but only at the highest elevations and east of these. We also find that the mountainous regions of Utah, Wyoming and Idaho in the northwestern border of the basin show strong decreasing snowfall. On the other hand, SFE/P shows significant declines for all regions (due to the increase in precipitation at higher elevations). We find a very robust signal showing the strongest decreasing trends in SFE at high elevations in the south and low elevations in the north. Our hypothesis for this trend is linked to the 0°C altitude-latitude variation. Precipitation phase will be most affected where this 0°C band relocates to higher elevations. The regions where winter temperatures hover well below this band will likely not experience this strong trend because snow will still form, and regions with average temperatures well above this band will still see most of their precipitation as rain, with the occasional (less frequent) snow. This physical mechanism agrees with arguments in the literature [*Dettinger and Cayan*, 1995; *Knowles et al.*, 2006; *Das et al.*, 2009; *Grundstein and Mote*, 2010; *Mote et al.*, 2008]. In general the previous studies find that middle altitudes are the most sensitive, here we argue that there is also a strong latitudinal component to the sensitivities, and southern regions within the basin experience strong snowfall trends at high elevations. If we plot the region where mean winter temperature is 0°C as a function of elevation and latitude, we see the clear migration into higher elevations and latitudes as we move into the future (Figure 10). Notably, the region where we see this migration coincides with the region of strongest negative trend in snowfall (shown as the contours in region in Figure 10). This work shows that the fraction of precipitation that falls as snow in the entire Colorado River Basin, and in particular the regions where mean winter temperatures are slightly below 0°C, will likely decrease. This has consequences, not only for the timing of streamflow, but also for ecological processes in these transitional zones.

[28] **Acknowledgments.** Francina Dominguez's work is supported by DOE (DE-SC0001172). We acknowledge Richard Jones and Wilfran Moufouma-Okia from the UK Met Office Hadley Centre for Climate Change for providing the HadCM3 forcing data for the WRF simulation. We acknowledge the modeling groups, the Program for Climate Model Diagnosis and Intercomparison (PCMDI) and the WCRP's Working Group on Coupled Modeling (WGCM) for their roles in making available the WCRP CMIP3 multimodel data set. This work has been partially founded by SAHRA (Center for Sustainability of semi-Arid Hydrology and Riparian Areas) under the STC Program of the National Science Foundation, Agreement EAR-9876800.

References

Barlage, M., F. Chen, M. Tewari, K. Ikeda, D. Gochis, J. Dudhia, R. Rasmussen, B. Livneh, M. Ek, and K. Mitchell (2010), Noah land surface model modifications to improve snowpack prediction in the Colorado Rocky Mountains, *J. Geophys. Res.*, *115*, D22101, doi:10.1029/2009JD013470.

Barnett, T. P., et al. (2008), Human-induced changes in the hydrology of the western United States, *Science*, *319*(5866), 1080–1083, doi:10.1126/science.1152538.

Bonfils, C., et al. (2008), Detection and attribution of temperature changes in the mountainous western United States, *J. Clim.*, *21*(23), 6404–6424, doi:10.1175/2008JCLI2397.1.

Burns, D., J. Klaus, and M. McHale (2007), Recent climate trends and implications for water resources in the Catskill mountain region, *J. Hydrol.*, *336*, 155–170, doi:10.1016/j.jhydrol.2006.12.019.

Castro, C., R. P. Pielke Sr., and G. Leoncini (2005), Dynamical downscaling: Assessment of value retained and added using the regional atmospheric modeling system (rams), *J. Geophys. Res.*, *110*, D05108, doi:10.1029/2004JD004721.

Chen, F., and J. Dudhia (2001), Coupling an advanced land surface-hydrology model with the Penn State-NCAR MM5 modeling system, Part I: Model implementation and sensitivity, *Mon. Weather Rev.*, *129*(4), 569–585.

Chou, M., and M. Suarez (1994), An efficient thermal infrared radiation parameterization for use in general circulation models, *NASA Tech. Memo. 104606*, 85 pp.

Christensen, N., and D. P. Lettenmaier (2007), A multimodel ensemble approach to assessment of climate change impacts on the hydrology and water resources of the Colorado River Basin, *Hydrol. Earth Syst. Sci.*, *11*, 1417–1434, doi:10.5194/hess-11-1417-2007.

Daly, C., R. Neilson, and D. Phillips (1994), A statistical-topographic model for mapping climatological precipitation over mountainous terrain, *J. Appl. Meteorol.*, *33*, 140–158.

Das, T., et al. (2009), Structure and detectability of trends in hydrological measures over the western United States, *J. Hydrometeorol.*, *10*(4), 871–892, doi:10.1175/2009JHM1095.1.

Dettinger, M., and D. Cayan (1995), Large-scale atmospheric forcing of recent trends toward early snowmelt runoff in California, *J. Clim.*, *8*(3), 606–623.

Dominguez, F., J. Canon, and J. Valdes (2009), IPCC-AR4 climate simulations for the southwestern US: The importance of future ENSO projections, *Clim. Change*, *99*(3–4), 499–514.

Dominguez, F., E. Rivera, D. P. Lettenmaier, and C. L. Castro (2012), Changes in winter precipitation extremes for the western United States under a warmer climate as simulated by regional climate models, *Geophys. Res. Lett.*, *39*, L05803, doi:10.1029/2011GL050762.

Gao, Y., J. A. Vano, C. Zhe, and D. P. Lettenmaier (2011), Evaluating climate change over the Colorado River basin using regional climate models, *J. Geophys. Res.*, *116*, D13104, doi:10.1029/2010JD015278.

Grundstein, A., and T. L. Mote (2010), Trends in average snow depth across the western United States, *Phys. Geogr.*, *31*(2), 172–185, doi:10.2747/0272-3646.31.2.172.

Hamlet, A., P. Mote, M. Clark, and D. Lettenmaier (2005), Effects of temperature and precipitation variability on snowpack trends in the western united states, *J Clim.*, *18*(21), 4545–4561.

Hidalgo, H. G., et al. (2009), Detection and attribution of streamflow timing changes to climate change in the western United States, *J. Clim.*, *22*(13), 3838–3855, doi:10.1175/2009JCLI2470.1.

Hong, S., J. Dudhia, and S. Chen (2004), A revised approach to ice microphysical processes for the bulk parameterization of clouds and precipitation, *Mon. Weather Rev.*, *132*, 103–120.

Ikeda, K., et al. (2010), Simulations of seasonal snowfall over Colorado, *Atmos. Res.*, *97*(4), 462–477.

Intergovernmental Panel on Climate Change (2007), *The Physical Science Basis. Contribution of Working Group I to the Fourth Assessment Report of the Intergovernmental Panel on Climate Change*, edited by S. Solomon et al., Cambridge Univ. Press, New York.

Janic, Z. (1990), The step-mountain coordinate: Physical package, *Mon. Weather Rev.*, *118*, 1429–1443.

Janic, Z. (1996), The surface layer in the NCEP eta model, in *11th Conference on Numerical Weather Prediction*, pp. 354–355, Norfolk, Va., Am. Meteorol. Soc., Boston, Mass., 19–23 Aug.

Janic, Z. (2002), Nonsingular implementation of the Mellor-Yamada level 2.5 scheme in the NCEP meso model, *NCEP Off. Note 437*, 61 pp.

Joseph, R., and S. Nigam (2006), ENSO evolution and teleconnections in IPCCs twentieth-century climate simulations: Realistic representation?, *J. Clim.*, *19*, 4360–4377.

Kain, J., and J. Fritsch (1993), Convective parameterization for mesoscale models: The Kain-Fritsch scheme. The representation of cumulus convection in numerical models, *Meteorol. Monogr. Am. Meteorol. Soc.*, *24*, 165–170.

Karoly, D., K. Braganza, P. Stott, J. Arblaster, G. Meehl, A. Broccoli, and K. Dixon (2003), Detection of a human influence on North American climate, *Science*, *302*(5648), 1200–1203.

Kendall, M. (1975), *Rank Correlation Methods*, 4th ed., Charles Griffin, London.

Knowles, N., M. D. Dettinger, and D. R. Cayan (2006), Trends in snowfall versus rainfall in the western United States, *J. Clim.*, *19*(18), 4545–4559.

Kunkel, K. E., et al. (2005), Quality control of pre-1948 cooperative observer network data, *J. Atmos. Ocean. Technol.*, *22*, 1691–1705.

Lettenmaier, D., E. Wood, and J. Wallis (1994), Hydro-climatological trends in the continental United States, 1948–88, *J. Clim.*, *7*, 586–607.

Leung, L., and Y. Qian (2003), The sensitivity of precipitation and snowpack simulations to model resolution via nesting in regions of complex terrain, *J. Hydrometeorol.*, *4*(6), 1025–1043.

Maurer, E. P., A. W. Wood, J. C. Adam, D. P. Lettenmaier, and B. Nijssen (2002), A long-term hydrologically based dataset of land surface fluxes and states for the conterminous United States, *J. Clim.*, *15*, 3237–3251.

Mearns, L., W. Gutowski, R. Jones, R. Leung, S. McGinnis, A. Nunes, and Y. Qian (2009), A regional climate change assessment program for North America, *EOS Trans. AGU*, *90*(36), 311.

Miguez-Macho, G., G. Stenchikov, and A. Robock (2004), Spectral nudging to eliminate the effects of domain position and geometry in regional climate model simulations, *J. Geophys. Res.*, *109*, D13104, doi:10.1029/2003JD004495.

Milly, P. C. D., K. A. Dunne, and A. V. Vecchia (2005), Global pattern of trends in streamflow and water availability on a changing climate, *Nature*, *438*(7066), 347, doi:10.1038/nature04312.

Mlawer, E., S. Taubman, P. Brown, M. Iancono, and S. Clough (1997), Radiative transfer for inhomogeneous atmosphere: RRTM, a validated correlated k model for the longwave, *J. Geophys. Res.*, *102*(D14), 16,663–16,682.

Mote, P., A. Hamlet, M. Clark, and D. Lettenmaier (2005), Declining mountain snow-pack in western North America, *Bull. Am. Meteorol. Soc.*, *86*(1), 39–49, doi:10.1175/BAMS-86-1-39.

Mote, P., A. Hamlet, and E. Salathe (2008), Has spring snowpack declined in the Washington cascades?, *Hydrol. Earth Syst. Sci.*, *12*(1), 193–206.

Pierce, D. W., et al. (2008), Attribution of declining western us snowpack to human effects, *J. Clim.*, *21*(23), 6425–6444, doi:10.1175/2008JCLI2405.1.

Rasmussen, R., et al. (2011), High-resolution coupled climate runoff simulations of seasonal snowfall over Colorado: A process study of current and warmer climate, *J. Clim.*, *24*, 3015–3048, doi:10.1175/2010JCLI3985.1.

Rio, S., L. Herrero, R. Fraile, and A. Penas (2010), Spatial distribution of recent rainfall trends in Spain (1961–2006), *Int. J. Climatol.*, *31*, 656–667, doi:10.1002/joc.2111.

Rockel, B., et al. (2008), Dynamical downscaling: Assessment of model system dependent retained and added variability for two different regional climate models, *J. Geophys. Res.*, *113*, D21107, doi:10.1029/2007JD009461.

Rose, S. (2009), Rainfall-runoff trends in the south-eastern USA: 1938–2005, *Hydrol. Processes*, *23*, 1105–1118, doi:10.1002/hyp.7177.

Rutter, N., et al. (2009), Evaluation of forest snow processes models (SnowMIP2), *J. Geophys. Res.*, *114*, D06111, doi:10.1029/2008JD011063.

Serreze, M. C., M. P. Clark, and R. L. Armstrong (1999), Characteristics of the western United States snowpack from snowpack telemetry (SNOTEL) data, *Water Resour. Res.*, *35*(7), 2145–2160.

Shepard, D. S. (1984), Computer mapping: The SYMAP interpolation algorithm, in *Spatial Statistics and Models*, edited by G. L. Gaile and C. J. Willmott, pp. 133–145, D. Reidel, Dordrecht, Netherlands.

Skamarock, W., J. Klemp, J. Dudhia, G. Gill, D. Barker, W. Wang, and J. Powers (2005), A description of the advanced research WRF version 2, *NCAR Tech. Note TN-468+STR*, 100 pp., Mesoscale and Microscale Meteorol. Div., Natl. Cent. for Atmos. Res., Boulder, Colo.

Stewart, I., D. Cayan, and M. Dettinger (2005), Changes toward earlier streamflow timing across western North America, *J. Clim.*, *18*(8), 1136–1155.

van Oldenborgh, G., S. Philip, and M. Collins (2005), El Nino in a changing climate: A multi-model study, *Ocean Sci.*, *1*, 81–95.

Wang, S., R. R. Gillies, E. S. Takle, W. J. Gutowski Jr. (2009), Evaluation of precipitation in the intermountain region as simulated by the NARCCAP regional climate models, *Geophys. Res. Lett.*, *36*, L11704, doi:10.1029/2009GL037930.

Wang, Z., X. Zeng, and M. Decker (2010), Improving snow processes in the Noah land model, *J. Geophys. Res.*, *115*, D20108, doi:10.1029/2009JD013761.

Xu, Z., K. Takeuchi, H. Ishidaira, and J. Li (2005), Long-term trend analysis for precipitation in Asian Pacific FRIEND river basins, *Hydrol. Processes*, *19*, 3517–3532, doi:10.1002/hyp.5846.

Zhang, X., K. Harvey, W. Hogg, and T. Yuzyk (2001), Trends in Canadian streamflow, *Water Resour. Res.*, *37*(4), 987–998, doi:10.1029/2000WR900357.

C. L. Castro and F. Dominguez, Department of Atmospheric Sciences, University of Arizona, 1118 E. 4th St., Tucson, AZ 85721, USA. (francina@hwr.arizona.edu)

H. F. Diaz, NOAA/ESRL/CIRES, 325 Broadway, Boulder, CO 80305, USA.

M. Durcik and J. Valdes, Department of Hydrology and Water Resources, University of Arizona, 1133 E. James E. Rogers Way, Tucson, AZ 85721, USA.

S. Wi, Department of Civil Engineering and Engineering Mechanics, University of Arizona, 1209 E. Second St., Tucson, AZ 85721, USA.